ELSEVIER

Urologic Oncology: Seminars and Original Investigations ▮ (2017) ▮▮▮–▮▮▮

UROLOGIC ONCOLOGY

Original article

Activation of the kynurenine pathway predicts poor outcome in patients with clear cell renal cell carcinoma

Giuseppe Lucarelli, M.D., Ph.D.[1,a,*], Monica Rutigliano, Ph.D.[a,1], Matteo Ferro, M.D.[b,1], Andrea Giglio, Ph.D.[a], Angelica Intini, Ph.D.[a], Francesco Triggiano, Ph.D.[a], Silvano Palazzo, M.D.[a], Margherita Gigante, Ph.D.[c], Giuseppe Castellano, M.D.[c], Elena Ranieri, Ph.D.[d], Carlo Buonerba, M.D.[e], Daniela Terracciano, Ph.D.[f], Francesca Sanguedolce, M.D.[g], Anna Napoli, M.D.[h], Eugenio Maiorano, M.D.[h], Franco Morelli, M.D.[i], Pasquale Ditonno, M.D.[a], Michele Battaglia, M.D.[a]

[a] *Department of Emergency and Organ Transplantation—Urology, Andrology and Kidney Transplantation Unit, University of Bari, Bari, Italy*
[b] *Department of Urology, European Institute of Oncology, Milan, Italy*
[c] *Department of Emergency and Organ Transplantation—Nephrology, Dialysis and Transplantation Unit, University of Bari, Bari, Italy*
[d] *Department of Medical and Surgical Sciences, Clinical Pathology Unit, University of Foggia, Foggia, Italy*
[e] *Department of Clinical Medicine, Medical Oncology Unit, Federico II University, Naples, Italy*
[f] *Department of Translational Medical Sciences, Federico II University, Naples, Italy*
[g] *Department of Pathology, University of Foggia, Foggia, Italy*
[h] *Department of Pathology, University of Bari, Bari, Italy*
[i] *Casa Sollievo della Sofferenza Hospital, Medical Oncology Unit, San Giovanni Rotondo, Italy*

Received 20 January 2017; received in revised form 17 February 2017; accepted 27 February 2017

Abstract

Objective: To investigate the expression of the kynurenine (KYN) pathway components and the prognostic role of the KYN-to-tryptophan ratio (KTR) in a cohort of patients with clear cell renal cell carcinoma (ccRCC).

Materials and methods: The expression of KYN pathway components was investigated by tissue microarray-based immunohistochemistry, indirect immunofluorescence, and confocal microscopy analysis in 100 ccRCC cases and 30 normal renal samples. The role of this pathway in sustaining cancer cell proliferation, migration, and chemoresistance was evaluated. In addition, tryptophan and KYN concentrations and their ratio were measured in serum of 195 patients with ccRCC using a sandwich enzyme-linked immunosorbent assay. The role of KTR as a prognostic factor for ccRCC cancer-specific survival (CSS) and progression-free survival (PFS) was assessed.

Results: Tissue microarray-based immunohistochemistry and indirect immunofluorescence staining showed an increased signal for KYN pathway components in ccRCC. Kaplan-Meier curves showed significant differences in CSS and PFS among groups of patients with high vs. low KTR. In particular, patients with high KTR values had a 5-year survival rate of 76.9% as compared with 92.3% for subjects with low levels ($P < 0.0001$). Similar findings were observed for PFS (72.8% vs. 96.8% at 5 y). At multivariate analysis, KTR was an independent adverse prognostic factor for CSS (hazard ratio $= 1.24$, $P = 0.001$), and PFS (hazard ratio $= 1.14$, $P = 0.001$).

Conclusions: The involvement of the KYN pathway enzymes and catabolites in ccRCC occurs via both immune and nonimmune mechanisms. Our data suggest that KTR could serve as a marker of ccRCC aggressiveness and as a prognostic factor for CSS and PFS.

Keywords: Renal cell carcinoma; Cancer metabolism; Kynurenine; Indoleamine 2,3-dioxygenase; Aryl hydrocarbon receptor

1. Introduction

Renal cell carcinoma (RCC) is one among the most common cancers in the United States, with 63,990 estimated new cases, and 14,400 estimated deaths in 2017 [1].

The pathogenesis of RCC is still poorly understood, although cigarette smoking, obesity, hypertension, diabetes,

This work was supported in part by a Grant from "Regione Puglia—ARTI" (Progetto FiR 4HE9F93 to G. Lucarelli—Intervento cofinanziato dal Fondo di Sviluppo e Coesione 2007–2013—APQ Ricerca Regione Puglia "Programma regionale a sostegno della specializzazione intelligente e della sostenibilità sociale ed ambientale—FutureInResearch").

[1] These authors have contributed equally to this study.

* Corresponding author. Tel./fax: +0039-080-547-8880.
E-mail address: giuseppe.lucarelli@inwind.it (G. Lucarelli).

http://dx.doi.org/10.1016/j.urolonc.2017.02.011
1078-1439/

and end-stage renal disease have been recognized as common risk factors [2–4]. In recent years, emerging evidence has confirmed that metabolic reprogramming is a cancer hallmark and has shown that many genes involved in the RCC pathogenesis play an important role in controlling cell metabolism [5–10]. Moreover, RCC is considered an immunogenic tumor on the basis of several observations that demonstrated a significant immune infiltrate in tumor stroma in association with T-cell dysfunction, the incidence of spontaneous regression, and a partial response to immunotherapy [11]. Multi-omics analysis of gene, protein, and metabolite expression profiles of biological specimens has led to the identification of potential biomarkers for early diagnosis, risk assessment, and outcome prediction, although none of these is currently recommended in clinical practice [12–14].

Tryptophan (TRP) is an essential amino acid that is metabolized by 3 main pathways: incorporation into proteins, serotonin production, and the formation of kynurenine (KYN) (Fig. 1A).

The conversion of TRP to KYN is mediated by 2 enzymes: indoleamine 2,3-dioxygenase (IDO1) and tryptophan 2,3-dioxygenase (TDO). Recently, a novel IDO1 paralogue has been discovered, named IDO2, whose role in TRP metabolism and cancer biology remains unclear. IDO1 expression, which is the rate-limiting enzyme for the TRP catabolism, can be induced in response to interferon (IFN)-gamma and tumor necrosis factor (TNF)-alpha stimulation.

In the past decade, many studies have shown that activation of this pathway plays an important role in cancer progression, through the action of 2 mechanisms, namely TRP depletion and the accumulation of immunosuppressive metabolites such as KYN [15]. In addition, a part of the protumorigenic role of KYN seems to be mediated by its interaction with the aryl hydrocarbon receptor (AhR) on immune and cancer cells [16].

In this study, we investigated the expression of the KYN pathway components in tissue specimens derived from patients with clear cell RCC (ccRCC), and characterized the IDO1+ circulating and tumor-infiltrating immune cells. We next evaluated the serum levels of TRP, KYN, TNF-α, and IFN-γ, and assessed the prognostic role of the KYN-to-TRP ratio (KTR) for ccRCC cancer-specific survival (CSS) and progression-free survival (PFS). Finally, we explored the possibility to target KYN/AhR axis to decreased cancer cell viability and migration, and increased sensitivity to chemotherapy.

2. Materials and methods

2.1. Metabolite extraction and chromatography/mass spectrometry of TRP and KYN

Primary renal tumor ($n = 40$) and nonneoplastic tissues ($n = 20$) were collected from 40 patients who underwent radical or partial nephrectomy for ccRCC. All tissue

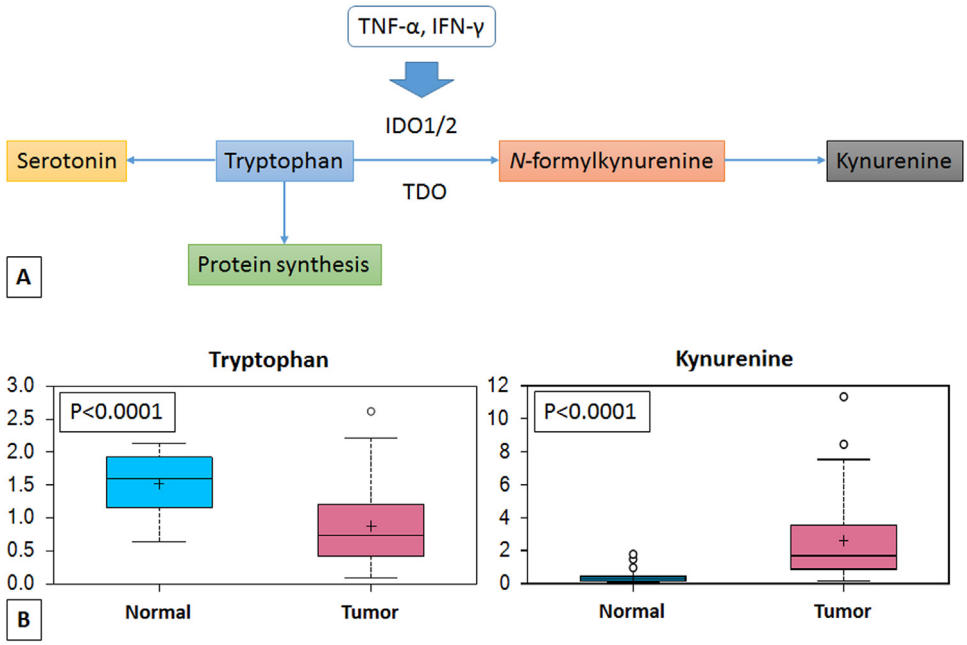

Fig. 1. (A) Tryptophan (TRP) metabolism. TRP is transformed to *N*-formylkynurenine by indoleamine 2,3-dioxygenase 1 (IDO1), IDO2, and tryptophan 2,3-dioxygenase (TDO). *N*-formylkynurenine is then degraded by formamidase to produce kynurenine. Tumor necrosis factor-α (TNF-α), and interferon-γ (IFN-γ) are the most important inducers of IDO1 expression. (B) Human kidney samples were obtained by nephrectomy and metabolites were extracted for metabolite profiling by LC/MS analysis. Tryptophan was reduced, whereas kynurenine was significantly increased in primary ccRCC (tumor) compared to benign kidney tissue (normal). *y*-axis: metabolite relative amount. LC/MS = liquid chromatography/mass spectrometry. (Color version of figure is available online.)

samples were maintained at −80°C until processed and prepared for the appropriate investigation, liquid chromatography/mass spectrometry or gas chromatography/mass spectrometry, as previously described [8].

2.2. Study population and tissue collection

Additionally, 60 primary renal tumor and 10 nonneoplastic tissues were collected from patients who underwent nephrectomy for ccRCC, for a total of 100 (40 + 60) ccRCC cases and 30 (20 + 10) normal renal samples. Two pathologists confirmed the presence of ccRCC in the neoplastic tissues and excluded tumor cells in the healthy specimens. In addition, serum samples were collected from 195 patients with ccRCC and 50 volunteers with no evidence of malignancy. Detailed clinical and pathological characteristics of the patients are summarized in Table 1. Tumor staging was reassigned according to the seventh edition of the AJCC-UICC TNM classification. The 2016 World Health Organization and Fuhrman classifications were used to attribute histological type and nuclear grade, respectively. Written informed consent to take part was given by all participants. The protocol for the research project has been approved by the local Ethics Committee and conforms to the provisions of the Declaration of Helsinki in 1995.

2.3. Serum TRP, KYN, TNF-α, and IFN-γ assay methods

Serum TRP, KYN, TNF-α, and IFN-γ levels were measured using a sandwich enzyme-linked immunosorbent assay according to the manufacturer's instructions.

Table 1
Clinical and pathological characteristics

Variable	n = 195
Age, y	
Median	60
95% CI	54–63
Sex	
Male	130 (67%)
Female	65 (33%)
Dimensions, cm	
Median	5.0
95% CI	4.7–5.5
Pathological stage	
pT1a	71 (36.5%)
pT1b	40 (20.5%)
pT2	43 (22%)
pT3	41 (21%)
pN+	32 (16.4%)
cM+	26 (13.3%)
Fuhrman grade	
G1–2	128 (65.6%)
G3–4	67 (34.3%)
Follow-up	
Median, mo	43
95% CI	38–45

2.4. Data mining using Oncomine gene expression microarray datasets and metabologram

IDO1, TDO, and AhR gene expressions were analyzed using microarray gene expression datasets deposited in the Oncomine database (https://www.oncomine.org/resource/login.html). In addition, the TRP metabolism was explored using the Metabologram data portal (http://sanderlab.org/kidneyMetabProject).

2.5. Immunohistochemistry and tissue microarray construction

High-density tissue microarrays were used for IDO1, TDO, AhR, and CD8 immunostaining. Archived formalin-fixed paraffin-embedded nephrectomy tissue samples for additional 60 primary renal tumor and 10 nonneoplastic tissues were obtained (for a total of 100 ccRCC cases and 30 normal renal samples). Protein immunoreactivity was scored on the extent and intensity of staining, which was graded on an arbitrary scale ranging from 0 to 3, with 0 = negative, 1 = low, 2 = medium, and 3 = high expression. The CD8+ infiltrating cells number was measured in at least 15 high power (×200) fields (hpf) by 2 independent observers.

2.6. Immunofluorescence and confocal laser scanning microscopy

Paraffin-embedded kidney sections were double-stained for IDO1, CD68, CD11c, NOS2, and CD163. The expression and localization of proteins was evaluated by indirect immunofluorescence and confocal microscopy analysis.

2.7. Primary cell cultures from renal tissues

Kidney epithelial tubular and neoplastic cells were isolated from tumor and normal kidney tissue specimens with EpCAM (CD326) Ab-conjugated magnetic microbeads (Miltenyi Biotec, Bergisch Gladbach, Germany), as previously described [17]. These cells were then characterized for EpCAM, CA IX, and AhR by immunocytochemistry to confirm their epithelial and renal lineage, and to evaluate the expression of KYN receptor.

2.8. Real-time polymerase chain reaction, wound healing, and cell viability assays

Refer to Supplementary Materials and Methods section for details.

2.9. Flow cytometry analysis

Peripheral blood mononuclear cells (PBMCs) from 10 patients with ccRCC and 4 age and sex–matched healthy controls were isolated by gradient centrifugation with

Histopaque 1077 (Sigma Aldrich). IDO1 staining was performed with unconjugated mouse monoclonal anti-IDO1 antibody (Abcam). Cells were first stained with Pc5.5-conjugated anti-CD14 (Beckman Coulter, Pasadena, CA) for 15 minutes at 4°C. Then cells were washed, fixed, permeabilized with BD Cytofix/Cytoperm Kit (BD Biosciences) and incubated for 20 minutes at room temperature with the primary antibody. Then cells were washed and incubated with the secondary antibody AlexaFluor 488 (Molecular Probes) for other 20 minutes. Data were obtained using a FC500 (Beckmann Coulter) flow cytometer and analyzed by Kaluza software. The area of positivity was determined using an isotype-matched monoclonal antibody. A total of 104 events for each sample were acquired.

2.10. Statistical analysis

Statistical calculations were performed with MedCalc 9.2.0.1 (MedCalc software, Mariakerke, Belgium) and PASW 18 software (PASW 18, SPSS, Chicago, IL, USA). Comparisons of median protein values between different groups were evaluated by Mann-Whitney *U* test. Receiver operating characteristic curve analysis was performed to identify the KTR cutoff for survival stratification.

In the CSS analysis, patients lost to follow-up, as well as patients who died of RCC-unrelated causes, were censored. PFS was calculated from the date of surgery to the date of disease recurrence. Disease progression was assessed radiographically (using computed tomography scan or magnetic resonance imaging) with a surveillance schedule based on EAU guidelines. Estimates of CSS and PFS were calculated according to the Kaplan-Meier method and compared with the log-rank test. Univariate and multivariate analyses were performed using the Cox proportional hazards regression model to identify the most significant variables for predicting CSS and PFS. A backward selection procedure was performed with removal criterion $P > 0.10$ based on likelihood ratio tests. Spearman's test was applied to evaluate the correlations between KTR and tumor stage/size. A $P < 0.05$ was considered statistically significant.

Additional details regarding the experimental procedures are provided in the Supplementary Materials and Methods section.

3. Results

3.1. Serum and tissue KYN levels are increased in ccRCC and KTR is a risk factor for ccRCC progression and mortality

We first analyzed 40 primary ccRCC vs. 20 normal renal tissues using an unbiased metabolomics profile (manuscript in preparation). This initial analysis identified statistically significant elevations of tissue KYN (greater than 5-fold) in ccRCC compared to normal parenchyma, in association with reduced levels of TRP (Fig. 1B).

Next, to evaluate the association between patients' survival and the expression levels of KYN, this metabolite was measured in serum of an independent cohort of 195 patients with ccRCC. As the serum KTR is a generally accepted clinical marker of IDO1 activity, this value was calculated for between-groups comparison and to classify the entire population by high ($\geq$4.5) vs. low KTR ($<$4.5) according to the cutoffs obtained with receiver operating characteristic curve analysis. Serum KYN levels and KTR were significantly higher in patients with RCC than in healthy subjects ($P < 0.0001$) (Fig. 2). Statistically significant differences resulted between KTR values and clinical stage ($P < 0.0001$; Spearman correlation, $r_s = 0.48$; $P < 0.0001$), tumor size ($r_s = 0.49$, $P < 0.0001$), Fuhrman grade ($P = 0.001$), lymph node involvement ($P < 0.0001$), and visceral metastases ($P < 0.0001$) (Fig. 3A).

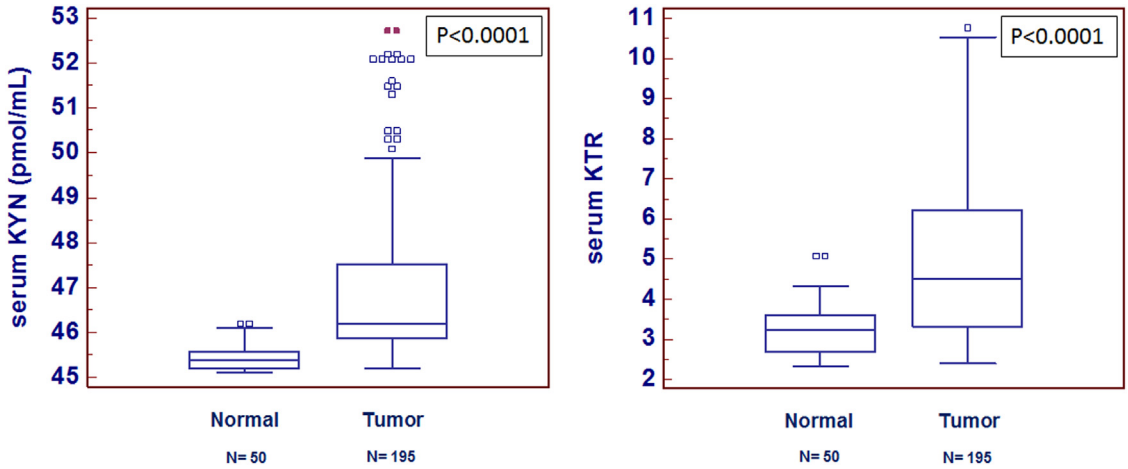

Fig. 2. Serum kynurenine (KYN) levels and kynurenine-to-tryptophan ratios (KTR) were significantly higher in patients with ccRCC than in healthy subjects. (Color version of figure is available online.)

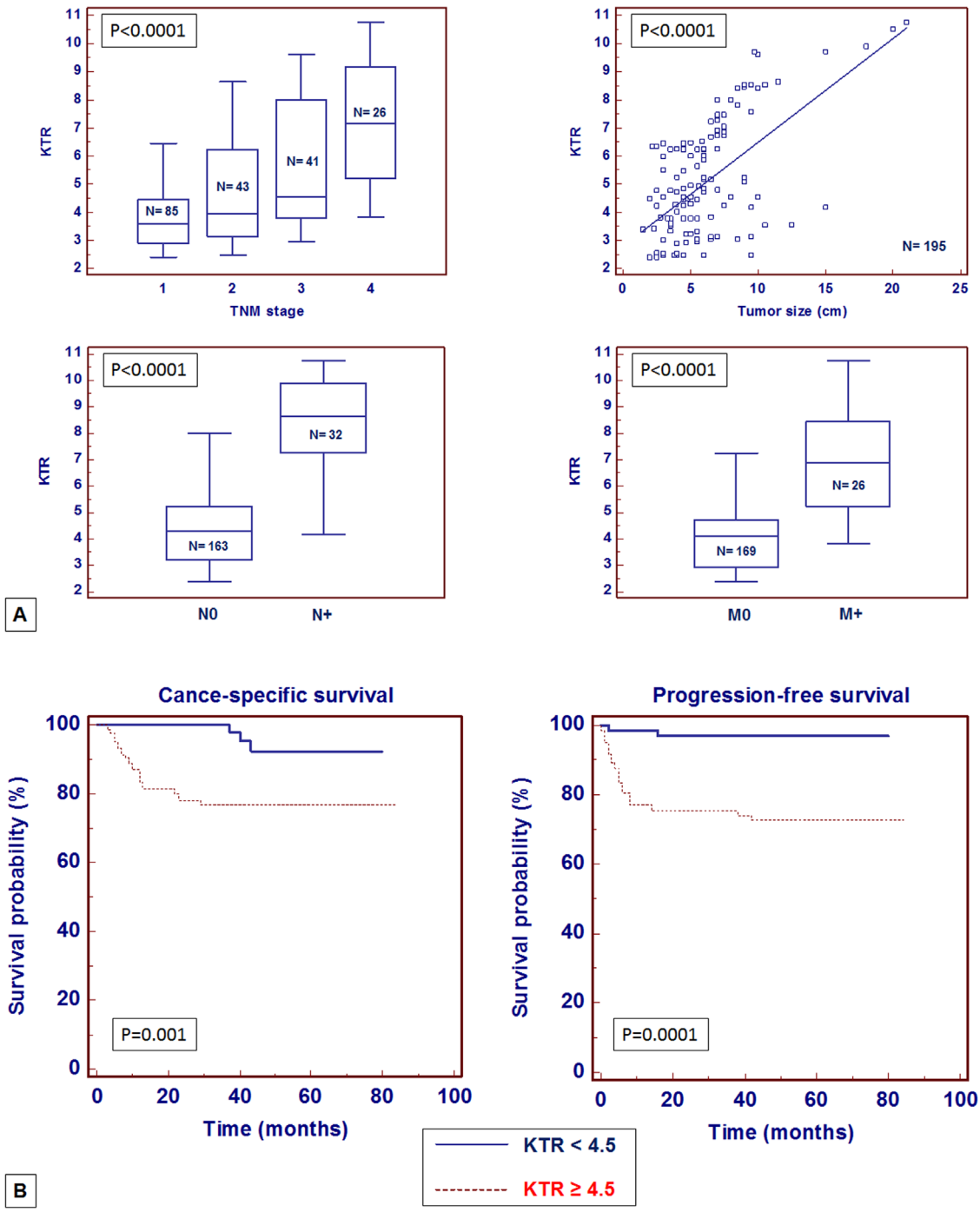

Fig. 3. (A) KTR median values were significantly higher in patients with advanced disease, larger tumor size, and with lymph node involvement and visceral metastases. (B) Kaplan-Meier cancer-specific survival (CSS) and progression-free survival (PFS) curves, stratified by KTR serum levels. Patients with higher KTR values had reduced CSS and PFS as compared to patients with lower values. (Color version of figure is available online.)

Kaplan-Meier survival curves for CSS and PFS, stratified by the KTR, are shown in Fig. 3B. After a median follow-up of 43 months (95% CI: 38–45), 29 patients had died of ccRCC, and 33 had disease progression. Both CSS and PFS were significantly decreased in patients with high KTR ($\geq$4.5). Univariate analysis for the predefined variables showed that pathological stage, presence of nodal and visceral metastases, Fuhrman grade, presence of necrosis, tumor size, and high KTR were significantly associated with the risk of death (Table 2) and progression (Table 3). At multivariate analysis by Cox regression modeling, pathological stage, presence of nodal and visceral metastases, Fuhrman grade, and high KTR, were independent adverse prognostic factors for CSS (Table 2) and PFS (Table 3).

Finally, as TNF-α and IFN-γ are the most important inducers of IDO1 expression under certain inflammatory

Table 2
Univariate and multivariate analyses for cancer-specific survival

Variable	Category	Univariate		Multivariate	
		HR (95% CI)	*P* value	HR (95% CI)	*P* value
T category	T3 vs. T1/2	3.81 (2.72–4.66)	0.002	2.12 (1.31–2.95)	0.01
N category	N+ vs. N0	5.71 (6.22–9.35)	0.001	4.25 (2.13–5.36)	0.001
M category	M+ vs. M0	8.21 (7.41–13.61)	0.001	5.12 (2.18–9.34)	0.001
Grade	G3/4 vs. G1/2	2.84 (1.13–5.61)	0.01	1.23 (1.01–2.16)	0.01
Necrosis	Yes vs. no	2.15 (1.25–3.76)	0.01	–	NS
Tumor size	Continuous	1.22 (1.11–1.56)	0.01	–	NS
KTR	Continuous	1.81 (1.20–2.11)	0.001	1.24 (1.02–1.97)	0.001

HR = hazard ratio; NS = not significant.

conditions, the serum levels of these cytokines were evaluated. We found lower levels of IFN-γ and higher levels of TNF-α in patients with ccRCC compared with healthy subjects (Fig. 4). In addition, TNF-α serum levels were correlated with KTR values ($r_s = 0.73$, $P < 0.001$).

3.2. IDO1 and AhR expressions are increased in renal tumor tissue

As IDO1 and TDO are the 2 rate-limiting enzymes of KYN formation, and this catabolite acts as an endogenous ligand for human AhR, we analyzed the transcription levels of these proteins in ccRCC tissue samples by quantitative real-time polymerase chain reaction. Normalized gene expression levels for IDO1 and AhR were significantly higher in the ccRCC compared with the normal tissue, whereas we did not find significant difference for TDO (Supplementary Fig. S1). To confirm the above findings, we analyzed the differential expression of IDO1, TDO, and AhR messenger RNA by data mining of the Oncomine microarray gene expression datasets (Supplementary Tables S1–S3). In accordance with our results, IDO1 and AhR were significantly up-regulated in ccRCC ($P = 0.002$ and $P = 0.001$, respectively). In addition, exploration of the Metabolgram Data Portal showed an abundance of KYN and the up-regulation of IDO1 when comparing tumors to normal kidney tissues (Supplementary Fig S2).

Next, to visualize the location and expression of IDO1, TDO, and AhR, we performed immunohistochemistry on normal and pathological tissues, using high-density tissue microarrays (Fig. 5A and B).

Normal kidney showed weak staining for AhR, predominantly localized in the renal tubule cell cytoplasm. Instead, pathological tissue showed a stronger staining in cancer cells, with a prevalently nuclear pattern. Similarly, IDO1 expression was very weak in normal kidney, but showed higher levels in ccRCC. Instead, TDO expression was very low both in cancer and normal tissue. Interestingly, the IDO1 signal was not identified in cancer cells but it was present in endothelial and tumor-infiltrating immune cells. Therefore, to differentiate dendritic cells from macrophages, we evaluated IDO1/CD11c and IDO1/CD68 coexpression in neoplastic tissue (Fig. 6). Immunofluorescence staining showed only a colocalized signal for both IDO1 and CD68 in infiltrating cells, demonstrating that these cells were macrophages (Fig. 6A). Next, to evaluate the macrophages polarization status, we studied the CD68/NOS2 (M1 macrophages) and CD68/CD163 (M2 macrophages) coexpression. We found that both tumor-associated macrophages (TAMs) polarization states were present in neoplastic tissue (Fig. 7).

Finally, as KYN pathway activation plays a role in regulating the antitumor response of the adaptive immune system, we evaluated the presence of CD8+ T cells in relation to tissue levels of KYN. We observed a reduced number of CD8+ T cells in renal cancers with higher levels of KYN compared to ccRCC cases with lower tissue values of this metabolite (Fig. 5C).

Table 3
Univariate and multivariate analyses for progression-free survival

Variable	Category	Univariate		Multivariate	
		HR (95% CI)	*P* value	HR (95% CI)	*P* value
T category	T3 vs. T1/2	4.22 (2.53–7.47)	0.001	3.21 (1.31–6.87)	0.01
N category	N+ vs. N0	3.41 (1.86–7.43)	0.01	2.16 (1.12–6.32)	0.01
M category	M+ vs. M0	5.06 (2.35–12.47)	0.001	3.89 (2.06–5.22)	0.001
Grade	G3/4 vs. G1/2	2.75 (1.12–6.01)	0.01	1.85 (1.01–2.91)	0.01
Necrosis	Yes vs. no	2.05 (1.12–2.96)	0.01	–	NS
Tumor size	Continuous	1.78 (1.12–2.37)	0.01	–	NS
KTR	Continuous	1.93 (1.12–2.45)	0.001	1.14 (1.02–1.85)	0.001

HR = hazard ratio; NS = not significant.

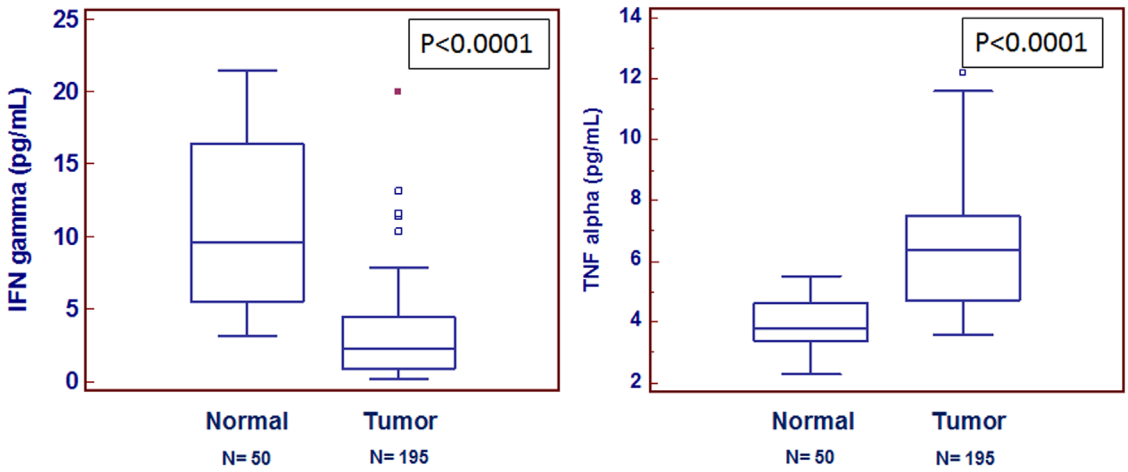

Fig. 4. Tumor necrosis factor-α (TNF-α), and interferon-γ (IFN-γ) were measured in serum of patients with ccRCC (tumor) and in controls (normal). Lower levels of IFN-γ and higher levels of TNF-α were found in patients with ccRCC compared with healthy subjects. (Color version of figure is available online.)

3.3. AhR has a role in cancer cell migration and decreases cisplatin-induced renal cancer cell death

To study the role of KYN/AhR axis in renal cancer cell migration and chemoresistance, in vitro assays were performed. In particular, the scratch wound healing assay showed that ccRCC cells treated with CH223191, an AhR antagonist, had decreased cell migratory characteristics compared with normal cells (Fig. 8). Next, we evaluated the role of AhR activation in reducing cisplatin-induced cytotoxicity. Normal and renal cancer cells were pretreated with CH223191. After cisplatin treatment, the death rate of tumor cells treated with CH223191 was significantly greater than that of untreated cancer cells ($P < 0.001$, Fig. 9A and B). MTT assay confirmed these findings by demonstrating decreased cell viability when tumor cells were pretreated with CH223191 before cisplatin incubation (69% at 1 h and 58% at 2 h) (Fig. 9C).

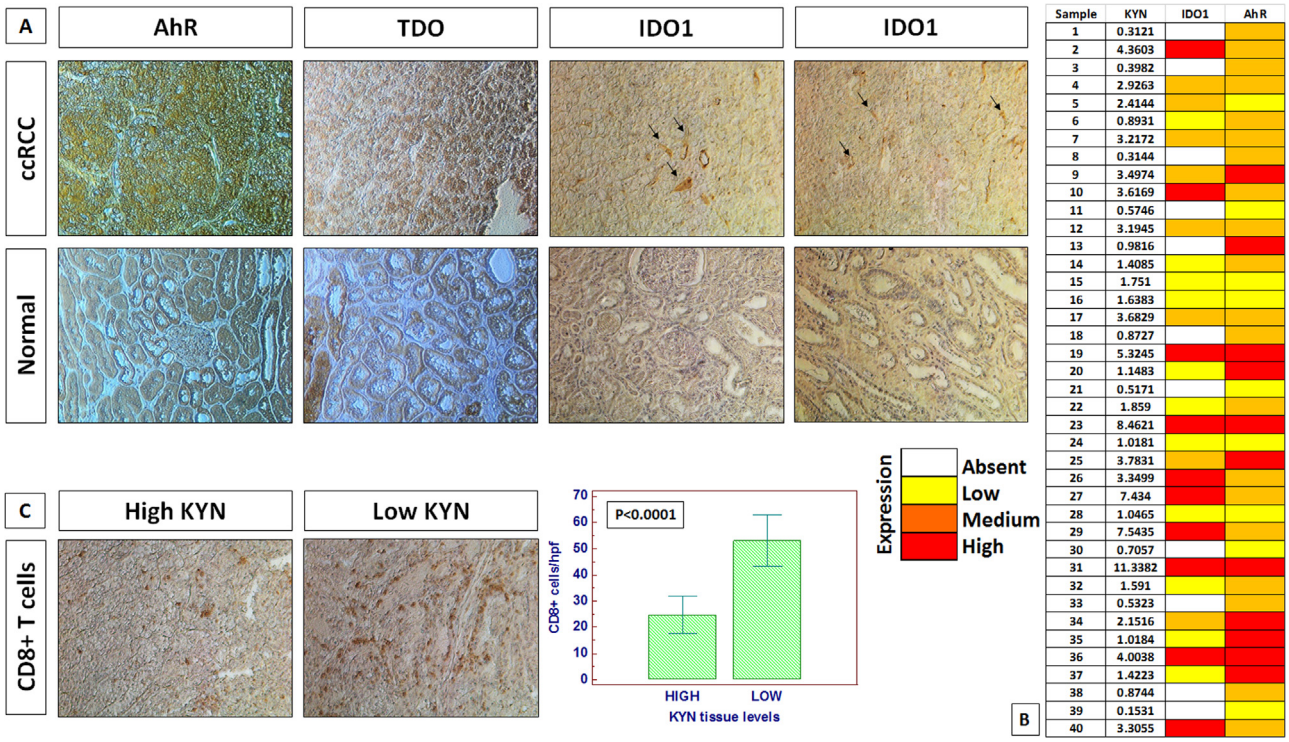

Fig. 5. (A) Immunohistochemical staining of AhR, TDO2, and IDO1 proteins in tissue microarrays of human ccRCC specimens. (B) Heat map summarizing AhR and IDO1 expression in 40 patients with ccRCC for which KYN tissue levels were available. (C) ccRCC specimens with high KYN tissue levels show a reduced number of infiltrating CD8+ T cells compared to tumors with low KYN values. Original magnification ×20. (Color version of figure is available online.)

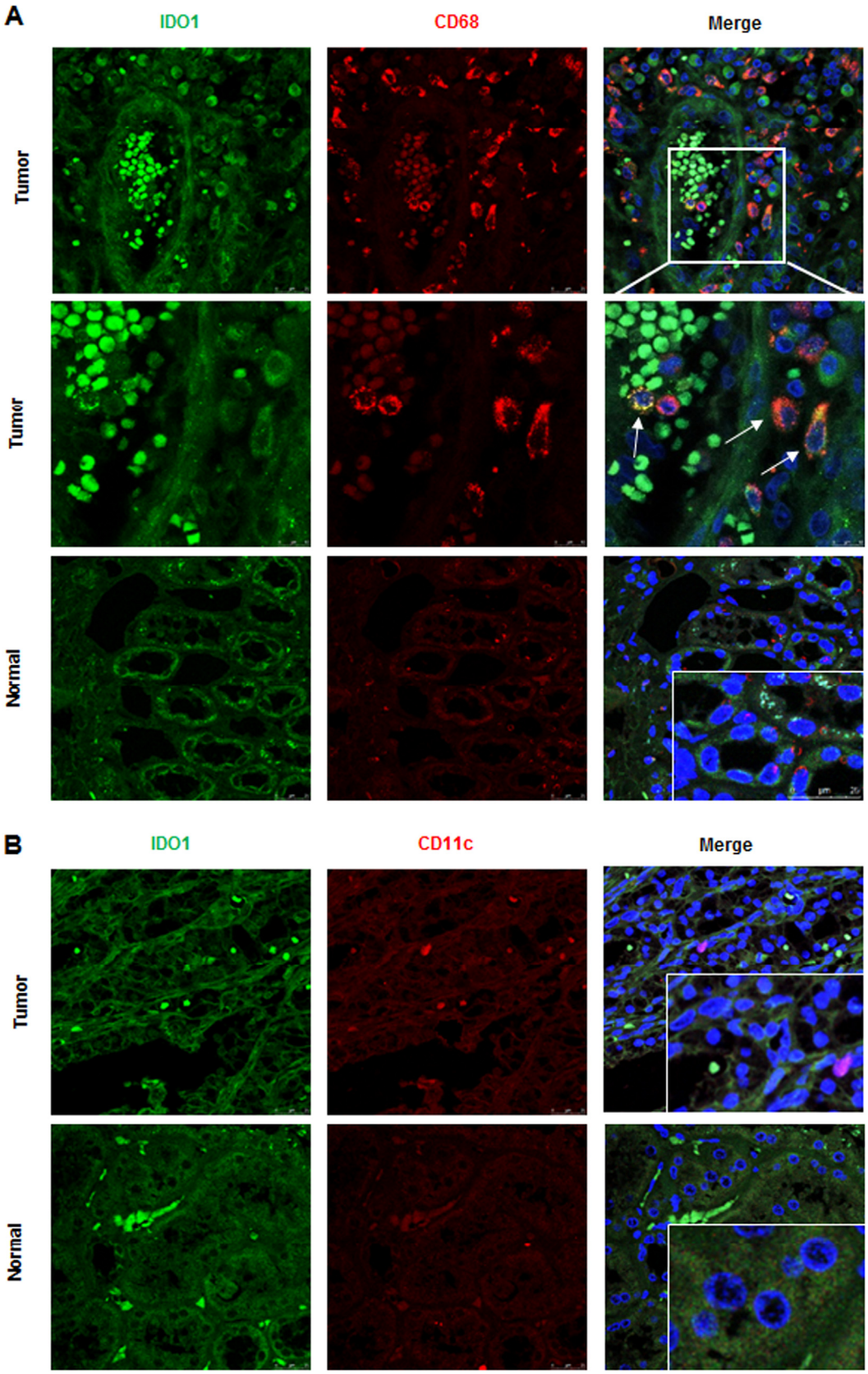

Fig. 6. Evaluation of IDO1+ tumor-infiltrating cells. To differentiate macrophages from dendritic cells, we evaluated IDO1/CD68 and IDO1/CD11c coexpression in neoplastic tissue. Immunofluorescence and confocal laser scanning microscopy demonstrated colocalization only for IDO1 and CD68 (A), whereas no colocalization was found for IDO1 and CD11c (B). (Color version of figure is available online.)

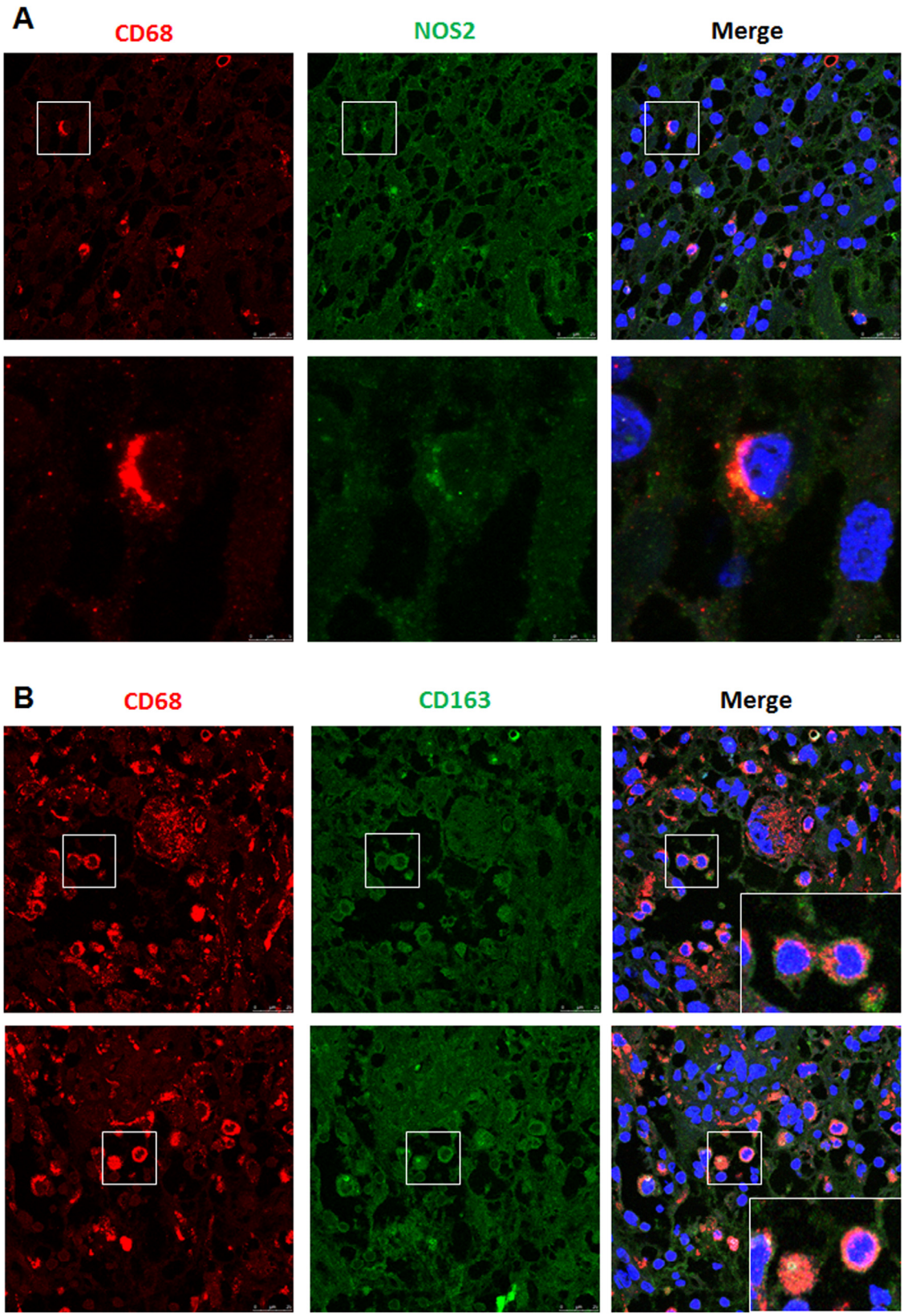

Fig. 7. To evaluate the macrophages polarization status, CD68/NOS2 (M1 macrophages—panel A) and CD68/CD163 (M2 macrophages—panel B) coexpressions were studied. Colocalization analysis showed that both tumor-associated macrophages (TAMs) populations were present in neoplastic tissue. (Color version of figure is available online.)

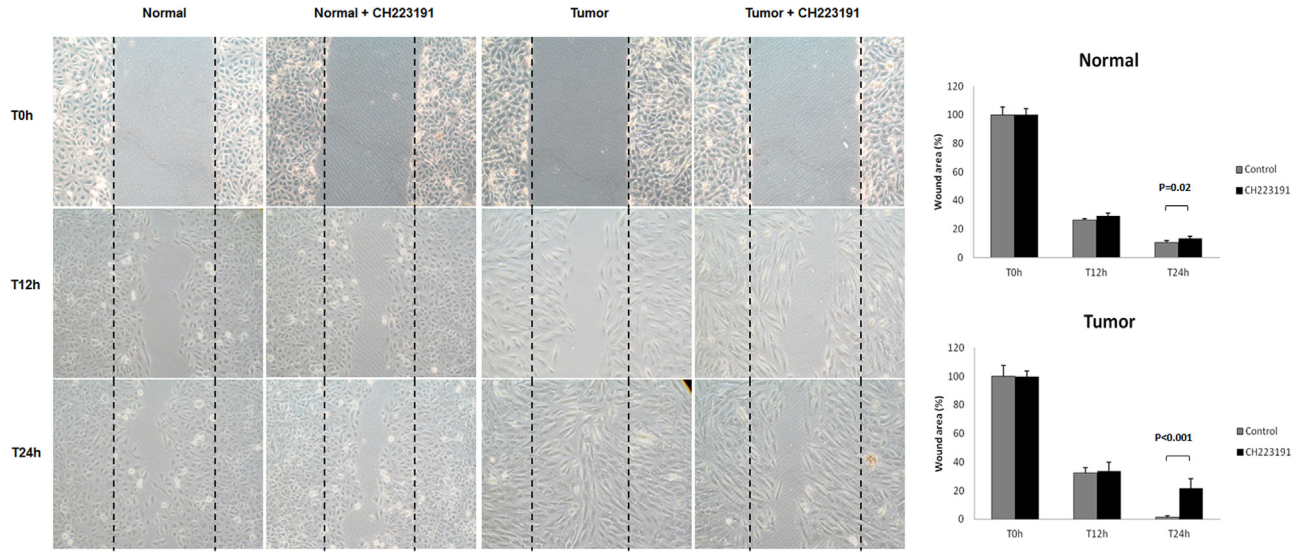

Fig. 8. Wounded normal and tumor cell monolayers were photographed 12 and 24 hours after the mechanical scratch and the area of the wounds was measured in 3 independent wound sites per group. When specified, the cells were exposed to 10 μM of CH223191 for 1 hour. RCC cells treated with CH223191 had decreased cell migratory capabilities compared with untreated tumor cells. (Color version of figure is available online.)

3.4. IDO1 expression in PBMCs

Flow cytometry was used to analyze the expression of IDO1 in freshly isolated PBMCs derived from patients with ccRCC with nonmetastatic vs. metastatic disease and compared with healthy controls. Considering the role of IDO1+ TAMs in ccRCC specimens, to analyze circulating monocytes, a gate was set around the CD14+ cells. We found a significant increase of circulating CD14+/IDO1-+ in patients with metastatic disease compared with patients with a localized tumor, as well as with healthy controls (Fig. 10).

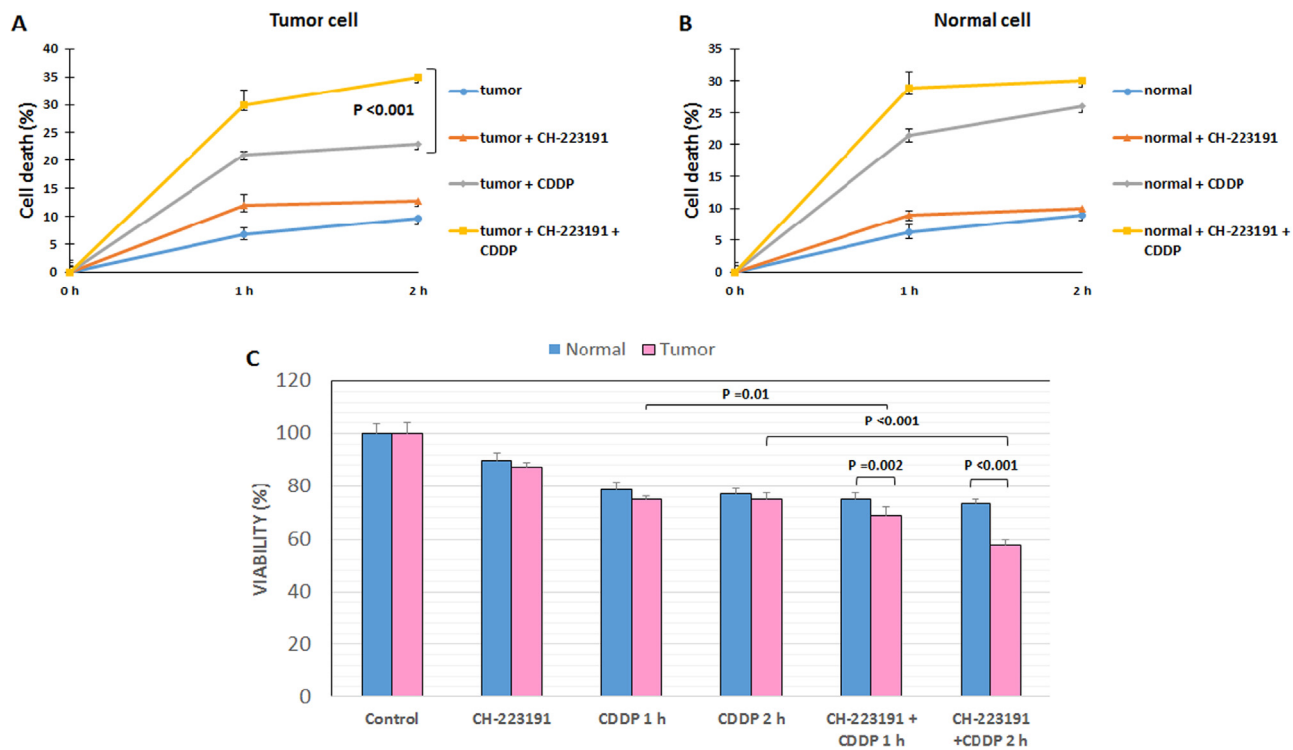

Fig. 9. AhR has a role in RCC resistance to cisplatin (CDDP)-induced cytotoxicity. (A) At 1 and 2 hours, the death rate of blocked tumor cells (tumor+CH223191+CDDP) was significantly higher than that of unblocked cells (tumor + CDDP) ($P < 0.001$). (B) No difference was observed between blocked (normal + CH223191 + CDDP) and unblocked (normal + CDDP) normal cells. (C) MTT assay revealed significantly decreased cell viability when renal tumor cells were pretreated with CH223191 before cisplatin incubation C. (Color version of figure is available online.)

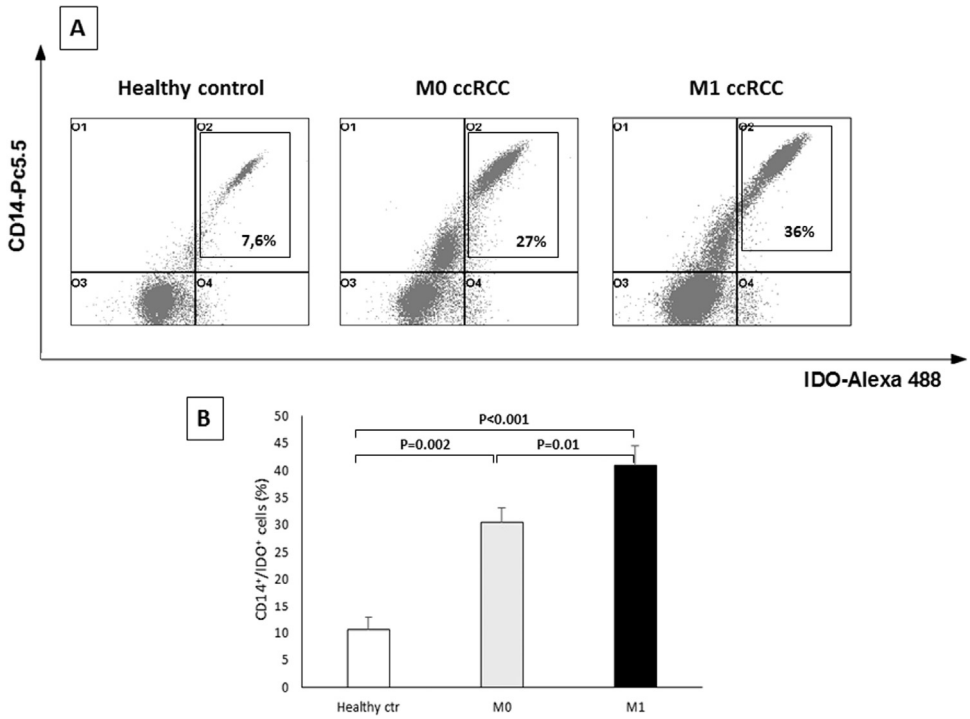

Fig. 10. Circulating IDO1+ CD14+ cells evaluated using flow cytometry on peripheral blood mononuclear cells. (A) A representative flow-cytometric analysis of one experiment is reported and the percentages of gated cells are shown. (B) Columns represent mean ± SD of IDO1+ CD14+ cells in healthy donors and in patients with nonmetastatic and metastatic ccRCC. SD = standard deviation.

4. Discussion

Many studies have shown that KYN pathway deregulation has a role in cancer progression and is negatively associated with patients' clinical outcome [18–20].

In the present study, we found that KYN was elevated nearly 6-fold in ccRCC tumor tissue, in association with reduced tissue levels of TRP. Therefore, to identify potential factors that could promote KYN accumulation in ccRCC, we initially analyzed the expression of the KYN-generating enzymes using quantitative real-time polymerase chain reaction and data mining of public Oncomine microarray datasets [21–25]. We found that only IDO1 mRNA was up-regulated in ccRCC, in association with the up-regulation of AhR, the widespread mediator of KYN action in tumor cells; these results were in accordance with a previous study that showed the existence of a mutually exclusive activation of IDO1 and TDO in cancer [16]. We next performed an immunohistochemical evaluation of protein expression and found that IDO1 was expressed in tumor endothelial cells, but especially in TAMs. The role of IDO1 in ccRCC endothelial cells was previously explored by Riesenberg et al. [26] who showed that tumors with a higher IDO-positive endothelial cells rate exhibited an increased microvascular density. TMAs are important regulators of the complex cross-talk between immune system and cancer cells. In agreement with recent studies that re-evaluated the TAM phenotypes beyond the M1/M2 polarization status [27], we found that both macrophages sub-populations were present in ccRCC and contributed to KYN production.

Opitz et al. [16] reported that KYN is an endogenous ligand of the AhR receptor, a cytoplasmic protein that moves into the nucleus, where it binds target genes and promotes tumor cell migration. We found that AhR was highly expressed in ccRCC, and its inhibition decreased cancer cell migratory capabilities in vitro. Cytotoxic chemotherapy has been largely ineffective in RCC. In recent years, an in-depth understanding of the molecular basis of ccRCC has led to the introduction of antiangiogenic therapies for this tumor, although these drugs yield partial responses in a minority of patients, with no evidence of complete responses [28,29]. Recent evidence suggested that AhR inhibition could increase sensitivity to chemotherapeutic drugs [30], so we hypothesized that AhR could be implicated in ccRCC chemoresistance. To explore this hypothesis, renal cancer cells were pretreated with CH223191, an AhR antagonist, and then incubated with cisplatin. Cisplatin was chosen for its broad-spectrum anticancer activity, and its inefficacy in ccRCC. After cisplatin incubation, the cell death rate of RCC cells treated with CH223191 was significantly higher than that of unblocked cancer cells, suggesting a role of the IDO1-KYN-AhR pathway in mediating a chemoresistance mechanism in ccRCC.

As the serum KTR is a generally accepted clinical marker of IDO1 activity, we evaluated this parameter in a cohort of patients with ccRCC compared to healthy individuals.

In particular, to address the significance of IDO1 activity in ccRCC prognosis, we stratified the patients' population according to KTR values. Kaplan-Meier curves showed significant differences in CSS and PFS between the patients groups with high vs. low KTR. Patients with high values of KTR had a 5-year survival rate of 76.9%, as compared to 92.3% for subjects with low levels ($P < 0.0001$). Similar findings were observed for PFS (72.8% vs. 96.8% at 5 y). These findings are in accordance with the results of other studies showing that high IDO1 activity contributes to the aggressive phenotype of different types of cancer [18–20].

Multivariate analyses demonstrated that high values of KTR (hazard ratio = 1.24, $P = 0.001$) together with pT-stage > 2, Fuhrman grade ≥3, and the presence of nodal and visceral metastases, were significantly predictive of the risk of death. Similarly, this parameter remained an independent prognosticator of outcome in PFS (hazard ratio = 1.14, $P = 0.001$). However, it must be pointed out that, although high values of KTR were significantly predictive of CSS and PFS, clinical factors such as pT-stage, N-stage, and M-stage were still much stronger predictors of poor outcomes than KTR.

Some studies have shown that high IDO1 activity is associated with increased tumor cell motility and metastatic potential. In agreement with these findings, we observed increased values of KTR in metastatic ccRCC compared to localized tumors. In particular, KTR values were significantly increased in patients with lymph node ($P < 0.0001$) and visceral metastases ($P < 0.0001$).

As TNF-α and IFN-γ are the most important cytokines involved in IDO1 expression, we evaluated the serum levels of these proteins in serum of patients with ccRCC. Interestingly, we found increased levels only of TNF-α, whereas IFN-γ values were significantly reduced in patients with cancer. Moreover, we observed an increased number of circulating IDO1+ monocytes in patients with advanced disease compared with patients with localized tumors and healthy individuals, suggesting that TNF-α could induce IDO1 in circulating monocytes, that successively populate tumor stroma as TAMs where they contribute to KYN production. Furthermore, TAMs could originate from tissue-resident macrophages arising from dedicated yolk sac progenitors [27]. In this setting, the generation of KYN, in association with TRP depletion, would cooperate with the low levels of IFN-γ to impair the antitumor response of the adaptive immune system. In fact, cytotoxic T cells were significantly reduced in tumors with higher tissue values of KYN. Therefore, according to this model that connects the metabolic deregulation with immune escape, the KYN produced by IDO1+ TAMs would not only impair the immunosurveillance by reducing the number of CD8+ T cells, but also by promoting cancer cells survival, migration, and chemoresistance through its interaction with AhR.

The main limitations of this study include the single-center design of the report, and its retrospective nature.

5. Conclusions

The involvement of the KYN pathway enzymes and catabolites in cancer occurs via both immune and non-immune mechanisms. In this study, we provide a detailed description of KYN pathway expression in ccRCC and discuss some clinical implications. In particular, we found that KTR could serve as a marker of ccRCC aggressiveness and as a prognostic factor for CSS and PFS. The inactivation of this pathway may serve as a novel therapeutic target.

Appendix A. Supporting information

Supplementary data associated with this article can be found in the online version at http://dx.doi.org/10.1016/j.urolonc.2017.02.011.

References

[1] Siegel RL, Miller KD, Jemal A. Cancer statistics, 2017. CA Cancer J Clin 2017;67:7–30.
[2] Hunt JD, van der Hel OL, McMillan GP, et al. Renal cell carcinoma in relation to cigarette smoking: meta-analysis of 24 studies. Int J Cancer 2005;114:101–8.
[3] Vavallo A, Simone S, Lucarelli G, et al. Pre-existing type 2 diabetes mellitus is an independent risk factor for mortality and progression in patients with renal cell carcinoma. Medicine (Baltimore) 2014;93:e183.
[4] Breda A, Lucarelli G, Rodriguez-Faba O, et al. Clinical and pathological outcomes of renal cell carcinoma (RCC) in native kidneys of patients with end stage renal disease: a long-term comparative retrospective study with RCC diagnosed in the general population. World J Urol 2015;33:1–7.
[5] Linehan WM, Srinivasan R, Schmidt LS. The genetic basis of kidney cancer: a metabolic disease. Nat Rev Urol 2010;7:277–85.
[6] Lucarelli G, Ferro M, Battaglia M. Multi-omics approach reveals the secrets of metabolism of clear cell-renal cell carcinoma. Transl Androl Urol 2016;5:801–3.
[7] Hsieh JJ, Cheng EH. The panoramic view of clear cell renal cell carcinoma metabolism: values of integrated global cancer metabolomics. Transl Androl Urol 2016;5(6):984–6.
[8] Lucarelli G, Galleggiante V, Rutigliano M, et al. Metabolomic profile of glycolysis and the pentose phosphate pathway identifies the central role of glucose-6-phosphate dehydrogenase in clear cell-renal cell carcinoma. Oncotarget 2015;6:13371–86.
[9] Hakimi AA, Reznik E, Lee CH, et al. An integrated metabolic atlas of clear cell renal cell carcinoma. Cancer Cell 2016;29:104–16.
[10] Lucarelli G, Rutigliano M, Sanguedolce F, et al. Increased expression of the autocrine motility factor is associated with poor prognosis in patients with clear cell-renal cell carcinoma. Medicine (Baltimore) 2015;94:e2117.
[11] Gigante M, Pontrelli P, Herr W, et al. miR-29b and miR-198 overexpression in CD8+ T cells of renal cell carcinoma patients down-modulates JAK3 and MCL-1 leading to immune dysfunction. J Transl Med 2016;14:84.
[12] Bui MH, Visapaa H, Seligson D, et al. Prognostic value of carbonic anhydrase IX and KI67 as predictors of survival for renal clear cell carcinoma. J Urol 2004;171:2461–6.
[13] Hsiao W, Herrel LA, Yu C, et al. Nomograms incorporating serum C-reactive protein effectively predict mortality before and after surgical treatment of renal cell carcinoma. Int J Urol 2015;22:264–70.

[14] Lucarelli G, Ditonno P, Bettocchi C, et al. Diagnostic and prognostic role of preoperative circulating CA 15-3, CA 125, and beta-2 microglobulin in renal cell carcinoma. Dis Markers 2014;2014: 689795.
[15] Platten M, Wick W, Van den Eynde BJ. Tryptophan catabolism in cancer: beyond IDO and tryptophan depletion. Cancer Res 2012;72: 5435–40.
[16] Opitz CA, Litzenburger UM, Sahm F, et al. An endogenous tumour-promoting ligand of the human aryl hydrocarbon receptor. Nature 2011;478:197–203.
[17] Galleggiante V, Rutigliano M, Sallustio F, et al. CTR2 identifies a population of cancer cells with stem cell-like features in patients with clear cell renal cell carcinoma. J Urol 2014;192:1831–41.
[18] Heng B, Lim CK, Lovejoy DB, et al. Understanding the role of the kynurenine pathway in human breast cancer immunobiology. Oncotarget 2016;7:6506–20.
[19] Palanichamy K, Thirumoorthy K, Kanji S, et al. Methionine and kynurenine activate oncogenic kinases in glioblastoma, and methionine deprivation compromises proliferation. Clin Cancer Res 2016; 22:3513–23.
[20] Stepien M, Duarte-Salles T, Fedirko V, et al. Alteration of amino acid and biogenic amine metabolism in hepatobiliary cancers: Findings from a prospective cohort study. Int J Cancer 2016;138:348–60.
[21] Gumz ML, Zou H, Kreinest PA, et al. Secreted frizzled-related protein 1 loss contributes to tumor phenotype of clear cell renal cell carcinoma. Clin Cancer Res 2007;13:4740–9.
[22] Beroukhim R, Brunet JP, Di Napoli A, et al. Patterns of gene expression and copy-number alterations in von-Hippel Lindau disease-associated and sporadic clear cell carcinoma of the kidney. Cancer Res 2009;69:4674–81.
[23] Jones J, Otu H, Spentzos D, et al. Gene signatures of progression and metastasis in renal cell cancer. Clin Cancer Res 2005;11: 5730–9.
[24] Lenburg ME, Liou LS, Gerry NP, et al. Previously unidentified changes in renal cell carcinoma gene expression identified by parametric analysis of microarray data. BMC Cancer 2003;3:1–19.
[25] Yusenko MV, Kuiper RP, Boethe T, et al. High-resolution DNA copy number and gene expression analyses distinguish chromophobe renal cell carcinomas and renal oncocytomas. BMC Cancer 2009;9:1–10.
[26] Riesenberg R, Weiler C, Spring O, et al. Expression of indoleamine 2,3-dioxygenase in tumor endothelial cells correlates with long-term survival of patients with renal cell carcinoma. Clin Cancer Res 2007;13:6993–7002.
[27] Ostuni R, Kratochvill F, Murray PJ, et al. Macrophages and cancer: from mechanisms to therapeutic implications. Trends Immunol 2015;36:229–39.
[28] Battaglia M, Lucarelli G. The role of renal surgery in the era of targeted therapy: the urologist′s perspective. Urologia 2015;82:137–8.
[29] Di Lorenzo G, De Placido S, Pagliuca M, et al. The evolving role of monoclonal antibodies in the treatment of patients with advanced renal cell carcinoma: a systematic review. Expert Opin Biol Ther 2016;16:1387–401.
[30] Stanford EA, Wang Z, Novikov O, et al. The role of the aryl hydrocarbon receptor in the development of cells with the molecular and functional characteristics of cancer stem-like cells. BMC Biol 2016;14:20.